



Influence of Argon Pressure on the Optical Bandgap Energy and Urbach tail of Sputtered Au/SiO₂ Nanocomposite Films

A. Belahmar, A. Chouiyakh

Department of Physics, Renewable Energy and Environment Laboratory, Faculty of Sciences, Ibn Tofail University, P.O. Box 133, 14000, Kenitra, Morocco

Abstract— Gold-silica nanocomposite thin films were deposited on glass substrate by RF-sputtering technique. X-ray diffraction (XRD) and optical transmission spectra were measured for investigating the influence of working argon pressure on the structural and optical properties of the Au/SiO₂ samples. The formation of Au NPs in the silica films is confirmed by XRD measurements. Effect of concentration of AuNPs on the optical properties of the Au/SiO₂ nanocomposite films, such as transmittance, optical absorption, optical gap energy (E_g) and Urbach tails (E_u) have been investigated using UV-VIS-NIR spectroscopy. The results show that all these parameters are affected by the deposition pressure. Hence, the transmittance decreased considerably in optical zone, the E_g increased from 4 eV to 4.22 eV and the E_u values change inversely with E_g , and decreased from 344meV to 192 meV, when the argon pressure increases. The best transparency of composite thin films is obtained at low argon pressure.

Keywords— Gold nanoparticles, Sputtering, Optical gap energy, Transmittance, Urbach tail.

I. INTRODUCTION

Nanocomposite films manufacturing by noble metal nanoparticles embedded in glass matrices has received special attention due to their notable optical properties owing to the surface plasmon resonance (SPR). The SPR absorption in noble metals at nanoscale have attracted significant attention due to their unique physicochemical properties, functionalities and high-speed optical communications properties as compared to their bulk counterparts. One of the most important aspect at the nanoscale is that the noble metals like silver and gold exhibit strong absorption band in visible range. The origin of this absorption is attributed due to their collective oscillation of conduction band electron in response to the electrical field of the electromagnetic radiation of light (e.g.[1]-[2]). The SPR wavelength of plasmonic materials critically depends on the size, shape, inter-particles separation, volume fraction of the metal and the dielectric constant of the embedding matrix (e.g.[3]-[7]).

Gold nanoparticles have attracted the attention of researchers because of their unique properties, and proven applicability in diverse areas such as medicine, catalysis, textile engineering, biotechnology, nano-biotechnology, bioengineering sciences, electronics (e.g.[8]-[19]). Silica is an excellent host matrix for growing small metallic particles. The metallic particles can be nucleated by heat or radiation, and grown at a high temperature, resulting in a very narrow size distribution inside the glass matrix (e.g.[20]). Silicon dioxide (SiO₂), one of the most abundant materials on Earth, has broadly used in various fields such as passivation layers of electronic devices, protection layers of magnetic or optical discs and anti-reflective coatings, because of their excellent chemical stability and optical transmittance with low refractive index (e.g.[21]-[22]).

Nanocomposite films consisting of metal particles such as gold embedded in a silica matrix have recently been the subject of many studies (e.g. [23]-[35]). A large number of methods have been used to obtain AuNPs embedded in SiO₂ films, such ion implantation (e.g. [36]-[37]), sol-gel (e.g.[38]), plasma enhanced chemical vapor deposition (PECVD) (e.g.[39]), hybrid techniques combining pulsed-DC sputtering and PECVD, which is used for simultaneous Au sputtering and SiO₂ deposition (e.g.[26]-[27]), and RF magnetron sputtering (e.g. [22],[23],[28],[29],[31],[32],[35],[40]-[42]). The flexibility and easy fabrication of diverse composite films are the advantages of sputtering method. The important factors to influence the formation of AuNPs are the working distance between the target and the substrate, rf-power, sputtering time, the substrate temperature, applied voltage, and working pressure.

The purpose of this work is to investigate the influence of variation argon pressure on the structural and optical properties of gold/silica composite films grown by RF-magnetron sputtering technique. The as-deposited films were characterized by X-ray diffraction and optical absorption spectroscopy.

II. EXPERIMENTAL METHODS

The samples, consisting of gold/silica composite thin films, were prepared by conventional radio-frequency magnetron sputtering method using an Alcatel SCM 650 apparatus. The target is constituted by two materials: a silica disc with a diameter of 50 mm was used as a target, over which chips of gold covering a fraction of the target area, were placed on top of silica disc. The deposition was accomplished on clean glass substrates at room temperature. The chamber was evacuated to a pressure better than 10⁻⁶mbar before the argon gas for the sputtering was introduced.

Deposition was carried out at a pressure over the range $2.10^{-3} - 5.10^{-3}$ mbar and the surface of gold/silica ratio, of materials from which the composite film fabricated is 2.6%. The relevant growth conditions of the films are shown in Table I.

Table I. Films Growth Conditions

Initial pressure (mbar)	1.10^{-6}
Working pressure (mbar)	$2.10^{-3} - 5.10^{-3}$
Au target (%)	2.6
Bias (V)	-50
Power (W)	50
Temperature	RT
Deposition time	4h30mn

Structural characterization of the obtained films was performed in a Philips PW 1710 spectrometer using Cu $K\alpha$ radiation $\lambda = 1.5406 \text{ \AA}$. The diffraction patterns were collected over the range 10° to 80° with 0.02 steps. The identification of Au crystalline phases was done using the JCPDS database cards (no. 04-0784). Optical absorption spectra of composite films were registered by a Shimadzu UV 30101 PC spectrometer, in near ultra-violet-visible-near infra-red range (NUV-VIS-NIR) from 200 to 2500 nm.

III. RESULTS AND DISCUSSION

3.1 Structural analysis

Fig. 1 shows the XRD patterns of the Au/SiO₂ composite films deposited at various argon pressures. X-ray diffractogram of gold thin film with a cubic structure, presented as a reference, is also reported in Fig. 1. It is evident that there are no Bragg reflections that are clearly visible in the spectra, due to the small AuNPs. Also, it well known that the peak centered on $2\theta=26^\circ$, in the spectra of all the samples, is attributed to the amorphous silica. It can be expected that the measured spectra of the composite films results from the superposition of two diffractograms, assigned to small gold particles and the amorphous silica matrix.

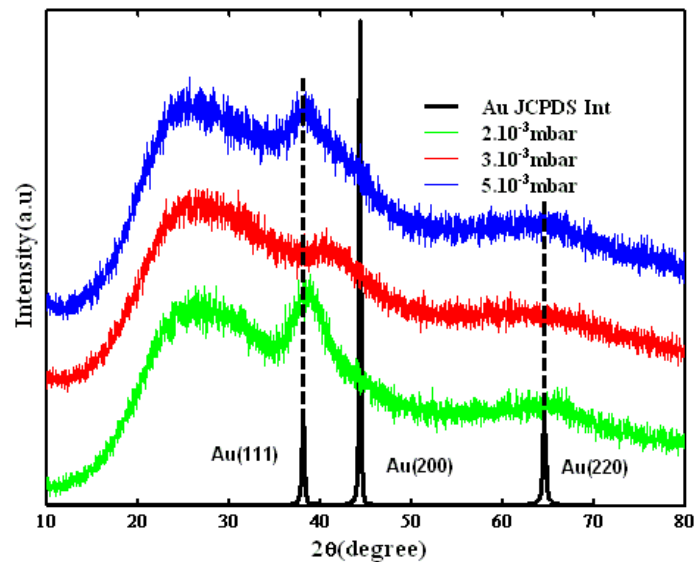


Fig. 1: XRD patterns of gold thin films Au/SiO₂ composite deposited with different Argon pressure and JCDPS of gold thin films.

To determine the phase structure, size, and lattice constant of AuNPs embedded in silica films, deconvolution procedure was used where details are reported elsewhere (e.g.[28]). The curve fitting of the XRD spectrum of the sample deposited at 2.10^{-3} mbar is reported in Fig. 2. From the values of the Bragg angle position θ_B and the full width at half maximum ($FWHM$) of the Au (111) reflection, we estimated the particle size (D) using the Debye-Scherrer's equation:

$$D = \frac{0.9 \lambda}{(FWHM) \cos \theta_B} \quad (1)$$

Where λ is the wavelength of $Cu_{K\alpha}$ radiation, θ_B is the Bragg angle of the diffraction peak. The average size of the AuNPs was found to be in the range $0.73 - 1.14$ nm. Also, from XRD analysis, it was observed that lattice parameter is lower than that of the gold bulk and thereby the presence of compressive volume strain in the AuNPs. Table II summarizes the fitting parameters determined from the Au (111) orientation plane for all the samples. It is important to note from the Table II that the lattice parameter of the particles increase regularly (Fig .3) and reach approximately the bulk value of 4.079 \AA at argon pressure of 5×10^{-3} mbar. This behavior has been reported in our previous work (e.g.[43]).

Table II. Results of the Curves Fitting of the Experimental Diffractograms of the Samples Deposited at Various Argon Pressures.

Argon pressure (mbar)	FWHM (degree)	2θ (degree)	Lattice parameter (Å)	size (Å)
2×10^{-3}	7.42	38.68	4.0318	11.35
3×10^{-3}	15.55	38.57	4.0429	5.41
5×10^{-3}	11.48	38.21	4.0795	7.33

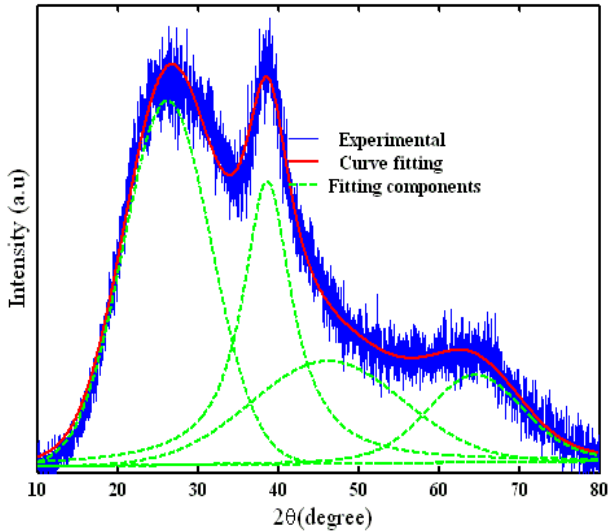


Fig. 2: Experimental diffractogram of Au /SiO₂ sample deposited at 2.10^{-3} mbar and their curve fitting where different pseudo-Voigt functions were taken into account.

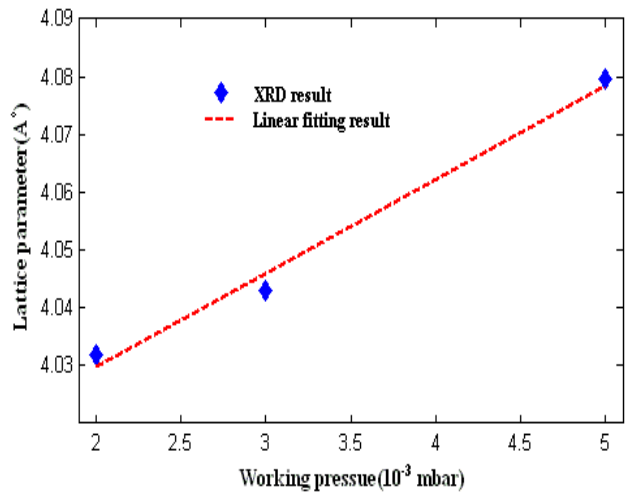


Fig. 3: variation of lattice parameter with working argon pressure

3.2 Optical studies

The transmittance in the UV-visible spectral ranges of the Au/SiO₂ composite thin films are shown in Fig. 3. The spectrum corresponding to the SiO₂ glass substrate is also presented as a reference. As can be seen, a strong transparent region between 1400 and 2000 nm, where the value of the transmission is of the order of 75% to 85% with a maximum value obtained for the sample deposited at argon pressure of 2.10^{-3} mbar. In this range of wavelengths, we also observe interference fringes. The presence of interferences implies that the Au/SiO₂ composite film has refractive index different from the silica glass, and these fringes are due to multiple reflections from the two interfaces of the film. This indicates that the films prepared under our conditions are smooth and uniform (e.g.[44]). Furthermore, with increasing argon pressure, we observe a decrease in the transmittance and a disappearance of the interference pattern in the films. It can be seen that for the wavelengths $\lambda < 500\text{nm}$, the optical absorption edge was shifted towards a shorter wavelength region when the argon pressure increases. However, for all the samples the transmission in the optical range (500 – 1000) nm is reduced, in comparison to the glass substrate. Thus, the Transmittance of the samples is sensitive to the variation of the Au concentration in the composite films. These results can give a design guide how to modify the optical transmission depending on metal/dielectric combination and deposition processes.

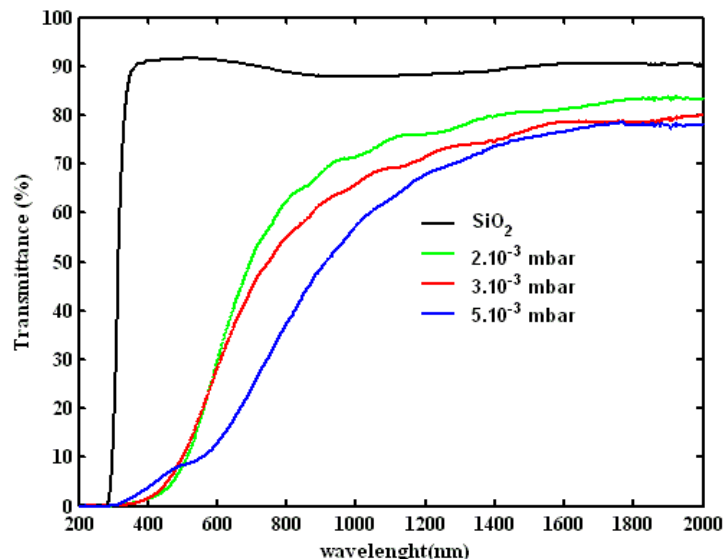


Fig. 4: Transmittance spectra of Au/SiO₂ composite films deposited at different Argon pressures.

Fig.5 shows the absorption spectra for all the samples deposited at various argon pressures. The curves display only an absorption edge and a weak and broad band, due to surface plasmon resonance, characteristic of small gold NPs in the case of the film deposited at an argon pressure of 5.10^{-3} mbar. Therefore, the position of the absorption edge can be controlled in both the near UV and whole visible band. Moreover, from the optical transmittance measurements we may calculate the absorption coefficient, α , of the films using the formula :

$$\alpha = \frac{\ln(100/T)}{d} \quad (2)$$

Where T is the transmittance, and d is the film thickness.

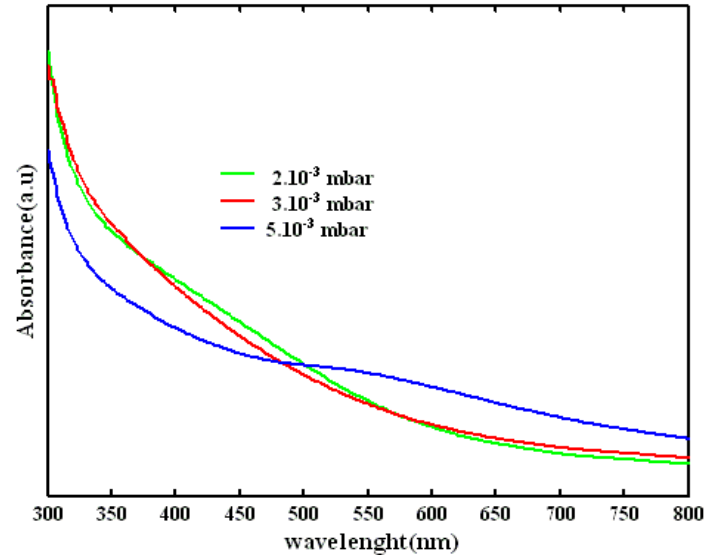


Fig. 5: Optical absorption spectra of Au/SiO₂ composite thin films deposited at different argon pressures .

The absorbance value in the edge region can be well determined by the optical absorption edge expression of the semiconductor with direct bandgap given by Tauc's relation (e.g[45]):

$$\alpha h\nu = B(h\nu - E_g)^{1/2} \quad (3)$$

Where $h\nu$ is the incident photon energy, E_g the optical band gap energy, and B is a constant. To determine the band gap energy of the Au/SiO₂ films, we use the intercept of $(\alpha h\nu)^2$ versus photon energy ($h\nu$) axis reported in Fig.6. The corresponding optical band gap energy obtained values, varied from 4eV to 4.22 eV, when the working argon pressure increased from 2.10^{-3} mbar to 5.10^{-3} mbar.

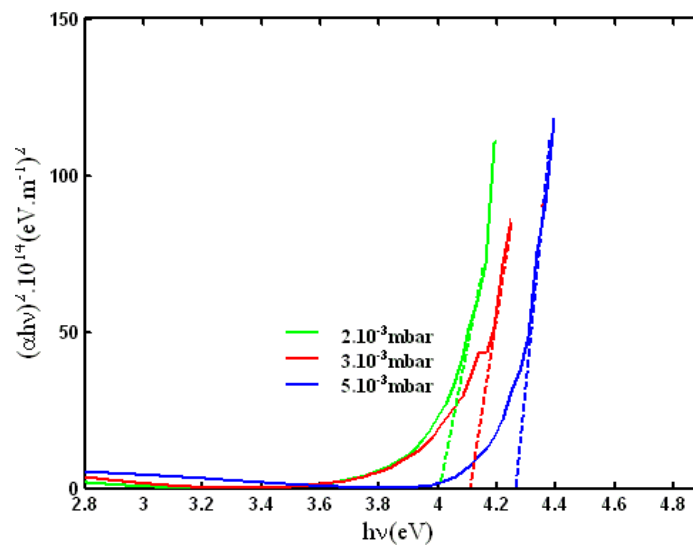


Fig. 6: Plot of $(\alpha h\nu)^2$ versus photon energy $h\nu$ for Au/SiO₂ deposited at different argon pressures.

Along the absorption coefficient curve and near the optical band edge there is an exponential part called Urbach tail. This exponential tail appears in the low crystalline, the disordered and amorphous materials. The variation of the absorption coefficient with the Urbach energy is given by the following equation (e.g.[46]):

$$\alpha = \alpha_0 \exp\left(-\frac{h\nu}{E_u}\right) \quad (4)$$

Where α_0 is a constant and E_u is the Urbach energy. We deduced the Urbach energy for the films from the plots of $\ln(\alpha)$ vs. $h\nu$. The value of E_u is calculated from the slope of the linear region of these curves varied from 344 meV to 192 meV .

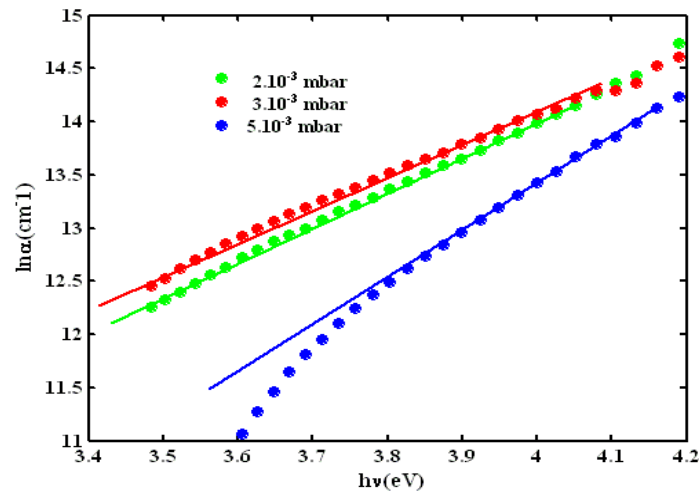


Fig. 7: A plot and linear fit of $\ln(\alpha)$ against the photon energy $h\nu$ for Au/SiO₂ deposited at different argon pressures.

We have plotted in Fig. 8 the value of E_g against E_u . It is noticed that as the value of E_u increases the bandgap decreases and there is a linear relation and correlation between them.

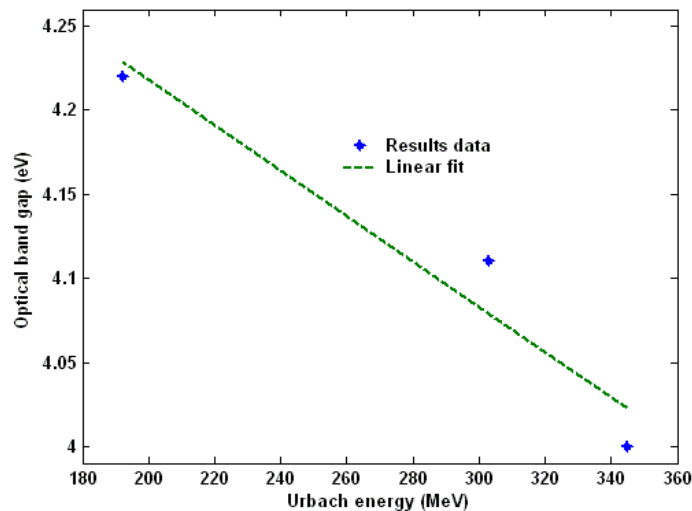


Fig. 8: The relation between the bandgap energy and the width of Urbach tail for Au/SiO₂ composite films deposited at different argon pressures

Taking the Urbach energy as an indicator of disorder in the material, the linear dependence, for the composite samples, between the later and the energy gap is an evidence that the value of E_g is probably set by the state of disorder or chemical composition, in comparison to the semiconductor thin films.

IV. CONCLUSION

Au/SiO₂ nanocomposite films have been prepared by RF-sputtering technique. The effect of argon pressure on the structural and optical properties of the composite films was investigated. XRD analysis shows that the lattice parameter of the Au NPs increase regularly and reach the bulk value. The transmittance measurements were taken at room temperature in the wavelength range 200–2000 nm. The absorption coefficient, optical gap energy and Urbach tail were deduced from the transmittance measurements. The increasing of the argon pressure decreases the disorder and it therefore increases the optical gap. A linear relationship was found between the bandgap energy and the width of Urbach tail. These results can give a design guide how to control the properties of composite films by metal nanoparticles, who can be used in diverse applications depending on metal/dielectric combination and deposition processes, like thermal solar conversion.

ACKNOWLEDGMENTS

We are grateful to Professor M.J.M. Gomes from the *Centre of Physics, University of Minho, Portugal*, for the experimental support.

REFERENCES

- [1] U. Kreibitz, M. Vollmer, *Optical Properties of Metal Clusters*, Springer, Berlin, 1995.
- [2] M. C. Mathpal, A. K. Tripathi, M. K. Singh, S. P. Gairola, S. N. Pandey, A. Agarwal, "Effect of annealing temperature on Raman spectra of TiO₂ nanoparticles," *Chemical Physics Letters*, vol. 555, pp. 182-186, 2013.

- [3] K.L. Kelly, E. Coronado, L.L. Zhao and G.C. Schatz, "The optical properties of metal nanoparticles: the influence of size, shape, and dielectric environment," *The Journal of Physical Chemistry. B*, vol. 107, pp. 668–677, 2003.
- [4] M.M. Miller, A.A. Lazarides, "Sensitivity of metal nanoparticle surface plasmon resonance to the dielectric environment," *The Journal of Physical Chemistry B*, vol.109, pp. 21556-21565, 2005.
- [5] D. Dalacu, L. Martinu, "Spectroellipsometric characterization of plasma-deposited Au/SiO₂ nanocomposite films," *Journal of Applied Physics*, vol.87, pp. 228-235, 2000.
- [6] C. Noguez, "Surface Plasmons on Metal Nanoparticles: The Influence of Shape and Physical Environment," *The Journal of Physical Chemistry C*, vol.111, pp. 3806-3819, 2007.
- [7] S. Link, M.A. EL-Sayed, "Shape and size dependence of radiative, non-radiative and photothermal properties of gold nanocrystals," *International Reviews in Physical Chemistry*, vol.19, pp. 409-453, 2000.
- [8] C.F. Bohren and D.R. Huffman, *Absorption and Scattering of Light by Small Particles*, John Wiley & Sons, Inc., New York, 1983.
- [9] J. Yguerabide and E.E. Yguerabide, "Light-scattering submicroscopic particles as highly fluorescent analogs and their use as tracer labels in clinical and biological applications," *Analytical Biochemistry*, vol. 262, pp. 137–156, 1998.
- [10] J. Yguerabide and E.E. Yguerabide, "Light-scattering submicroscopic particles as highly fluorescent analogs and their use as tracer labels in clinical and biological applications: Experimental characterization," *Analytical Biochemistry*, vol. 262, pp. 157–176, 1998.
- [11] V. Degiorgio and R. Piazza, "Light scattering in colloid and interface science," *Current Opinion in Colloid and Interface Science*, vol. 1, pp. 11–16, 1996.
- [12] R. Sardar, A.M. Funston, P. Mulvaney and R.W. Murray, "Gold nanoparticles: past, present, and future," *Langmuir*, vol. 25, pp. 13840–13851, 2009.
- [13] K. Kneipp, H. Kneipp, I. Itzkan, R.R. Dasari and M.S. Feld, "Ultrasensitive chemical analysis by Raman spectroscopy," *Chemical Reviews*, vol. 99, pp. 2957–2976, 1999.
- [14] I. Delfino, A.R. Bizzarri and S. Cannistraro, "Single-molecule detection of yeast cytochrome c by surface-enhanced Raman spectroscopy," *Biophysical Chemistry*, vol. 113, pp. 41–51, 2005.
- [15] I. Delfino, A.R. Bizzarri and S. Cannistraro, "Time-dependent study of single-molecule SERS signal from yeast cytochrome c," *Chemical Physics*, vol. 326, pp. 356–362, 2006.
- [16] S.E. Lohse and C.J. Murphy, "Applications of colloidal inorganic nanoparticles: from medicine to energy," *Journal of the American Chemical Society*, vol. 134, pp. 15607–15620, 2012.
- [17] K. Saha, S.S. Agasti, C. Kim, X. Li and V.M. Rotello, "Gold nanoparticles in chemical and biological sensing," *Chemical Reviews*, vol. 112, pp. 2739–2779, 2012.
- [18] A. Liang, Q. Liu, G. Wen and Z. Jiang, "The surface-plasmon-resonance effect of nanogold/silver and its analytical applications," *TRAC Trends in Analytical Chemistry*, vol. 37, pp. 32–47, 2012.
- [19] P.K. Jain, K.S. Lee, I.H. El-Sayed and M.A. El-Sayed, "Calculated absorption and scattering properties of gold nanoparticles of different size, shape, and composition: applications in biological imaging and biomedicine," *The Journal of Physical Chemistry. B*, vol. 110, pp. 7238–7248, 2006.
- [20] J. Rozra, I. Saini, S. Aggarwal, A. Sharma, "Spectroscopic analysis of Ag nanoparticles embedded in glass," *Advanced Materials Letters*, vol. 4, pp. 598-604, 2013.
- [21] K. Toki, K. Kusakabe, T. Odani, S. Kobuna, Y. Shimizu, "Deposition of SiO₂ and Ta₂O₅ films by electron-beam-excited plasma ion plating," *Thin Solid Films*, vol.281–282, pp. 401–403, 1 August 1996.
- [22] T. Oyama, H. Ohsaki, Y. Tachibana, Y. Hayashi, Y. Ono, N. Horie, "A new layer system of anti-reflective coating for cathode ray tubes," *Thin Solid Films*, vol.351, pp. 235–240, 30 August 1999.
- [23] H.B.Liao, R.F. Xiao, J.S. Fu, P. Yu, G.K. Wong, P. Sheng, "Large third-order optical nonlinearity in Au:SiO₂ composite films near the percolation threshold," *Appl. Phys. Lett.*, vol. 70, pp. 1–3, 1997.
- [24] I. Tanahashi, Y. Manabe, T. Tohda, S. Sasaki, A. Nakamura, "Optical nonlinearities of Au/SiO₂ composite thin films prepared by a sputtering method," *J. Appl. Phys.*, vol.79, pp.1244-1249, 1996.
- [25] D. Dalacu and L. Martinu, "Temperature Dependence of the Surface Plasmon Resonance in Au/SiO₂ Films," *Appl. Phys. Lett.*, vol.77, pp.4283-4285, 2000.
- [26] C.H. Kerboua, J.M. Lamarre, L. Martinu, S. Roorda, "Deformation, alignment and anisotropic optical properties of gold nanoparticles embedded in silica," *Nucl. Instrum. Methods Phys. Res. B*, vol.257, pp.42-46, 2007
- [27] J.M. Lamarre, Z. Yu, C. Harkati, S. Roorda, L. Martinu, "Optical and Microstructural Properties of Nanocomposite Au/SiO₂ Films Containing Particles Deformed by Heavy Ion Irradiation," *Thin Solid Films*, vol. 479, pp. 232-237, 2005.
- [28] A. Belahmar, A. Chouiyakh, "Effect of post-annealing on structural and optical properties of gold nanoparticles embedded in silica films grown by RF- sputtering," *Adv. in Phys. Theor. and Appl.*, vol.15, pp.38-46, 2013.
- [29] K.H Jung, J.W. Yoon, N. Koshizaki, Y.S. Kwon, "Fabrication and characterization of Au/SiO₂ nanocomposite films grown by radio-frequency cosputtering," *Curr. Appl. Phys.*, vol. 8, pp. 761–765, 2008.
- [30] G.Q. Yu, B.K. Tay, Z.W. Zhao, X.W. Sun, Y.Q. Fu, "Ion beam co-sputtering deposition of Au/SiO₂ nanocomposites," *Phys. E. Low-dim. Sys. and Nanostr.*, vol.27, pp. 362–368, 2005.

- [31] B. Zhuo, Y. Li, S. Teng, A. Yang, "Fabrication and Characterization of Au/SiO₂ nanocomposite films," *Appl. Surf. Sci.*, vol.256, pp. 3305–3308, 2010.
- [32] P. Sangpour, O. Akhavan, A.Z. Moshfegh, M. Roozbehi, "Formation of gold nanoparticles in heat-treated reactive co-sputtered Au-SiO₂ thin films," *Appl. Surf. Sci.*, vol.254, pp. 286–290, 2007.
- [33] S. Cho, H. Lim, K.S. Lee, T.S. Lee, B. Cheong, W.M. Kim, S. Lee, "Spectro-ellipsometric studies of Au/SiO₂ nanocomposite films," *Thin Sol. Films.*, vol. 475, pp. 133– 138, 2005.
- [34] M.S. Kennedy, N.R. Moody, D.P. Adams, M. Clift, D.F.Bahr, "Environmental influence on interface interactions and adhesion of Au/SiO₂," *Mat. Sci. and Engin. A* .vol.493 ,pp.299–304, 2008.
- [35] F. Ruffino, M.G. Grimaldi, C. Bongiorno, F. Giannazzo, F. Roccaforte, V. Raineri, "Microstructure of Au nanoclusters formed in and on SiO₂," *Superl. and Microstructu.*, vol.44 ,pp. 588–598, 2008.
- [36] K. Takahiro, S. Oizumi, K. Morimoto, K. Kawatsura, T. Isshiki, K. Nishio, et al, "Application of X-ray photoelectro spectroscopy to characterization of Au nanoparticles formed by ion implantation into SiO₂," *Appl. Surf. Sci.* vol.256, pp.1061-1064, 2009.
- [37] T. Cesca, C. Maurizio, B. Kalinic, C. Scian, E. Trave, G. Battaglin, P. Mazzoldi, G. Mattei, "Luminescent ultra-small gold nanoparticles obtained by ion implantation in silica," *Nucl. Instr. Meth. Phys. Res. Sec. B: Beam Inter. Mater. Atoms*, vol. 326, pp. 7-10, 2014.
- [38] M.C. Ferrara, L. Mirengi, A. Mevoli, L. Tapfer, "Synthesis and characterization of sol-gel silica films doped with size-selected gold nanoparticles," *Nanotech.*, vol. 19 , pp.65706-65714, 2008.
- [39] F. Ruffino, C. Bongiorno, F. Giannazzo, F. Roccaforte, V. Raineri, M.G. Grimaldi, "Effect of surrounding environment on atomic structure and equilibrium shape of growing nanocrystals: gold in/on SiO₂," *Nanosc. Res. Lett.*, vol. 2, pp. 240-247, 2007.
- [40] H.B. Liao, W. Weijia, G.K.L. Wong, "Preparation and optical characterization of Au/SiO₂ composite films with multilayer structure," *J. Appl. Phys.*, vol. 93, pp. 4485-4488, 2003.
- [41] [S. Debrus, J. Lafait, M. May, N. Pinçon, D. Prot, C. Sella, J. Venturini, "Z-scan determination of the third-order optical nonlinearity of gold: silica nanocomposites," *J. Appl. Phys.*, vl. 8 , pp. 4469-4475, 2000.
- [42] N. Pinçon, B. Palpant, D. Prot, E. Charron, S. Debrus, "Third-order nonlinear optical response of Au:SiO₂ thin films: Influence of gold nanoparticle concentration and morphologic parameters," *Eur. Phys. J. D*, vol.19 ,pp. 395-402, 2002.
- [43] A. Belahmar, A. Chouiyakh, "Influence of the Fabrication Conditions on the Formation and Properties of Gold Nanoparticles in Alumina Matrix Produced by Cosputtering," *International Journal of Nano and Material Sciences*, vol.3, pp.16-29, 2014.
- [44] N. Zebbar, M.S. Aida, A.E.K. Hafdallah, O. Daranfah, H. Lekiket, M. Kechouane, "Properties of ZnO Thin Films Grown on Si Substrates by Ultrasonic Spray and ZnO/Si Heterojunctions ," *Materials Science Forum*, Vol. 609, pp. 133-137, 2009 .
- [45] J. Tauc, R. Grigorovici, A. Vancu, "Optical properties and electronic structure of amorphous germanium," *physic. status solidi. (b)*, vol.15, pp.627-637, 1966.
- [46] F.Urbach , "The Long-Wavelength Edge of Photographic Sensitivity and of the Electronic Absorption of Solids," *J. Phys. Rev.*, vol. 9, pp.1324, 1953.